Lower hybrid current drive and ion cyclotron range of frequencies heating experiments in H-mode plasmas in Experimental Advanced Superconducting Tokomak

X. J. Zhang, B. N. Wan, Y. P. Zhao, B. J. Ding, G. S. Xu, X. Z. Gong, J. G. Li, Y. Lin, G. Taylor, J. M. Noterdaeme, F. Braun, S. Wukitch, R. Magne, X. Litaudon, R. Kumazawa, H. Kasahara, and EAST Team

Citation: Physics of Plasmas (1994-present) **21**, 061501 (2014); doi: 10.1063/1.4884356
View online: http://dx.doi.org/10.1063/1.4884356
View Table of Contents: http://scitation.aip.org/content/aip/journal/pop/21/6?ver=pdfcov
Published by the AIP Publishing

Lower hybrid current drive and ion cyclotron range of frequencies heating experiments in H-mode plasmas in Experimental Advanced Superconducting Tokomak

X. J. Zhang,[1] B. N. Wan,[1,a)] Y. P. Zhao,[1] B. J. Ding,[1] G. S. Xu,[1] X. Z. Gong,[1] J. G. Li,[1] Y. Lin,[2] G. Taylor,[3] J. M. Noterdaeme,[4,5] F. Braun,[4] S. Wukitch,[2] R. Magne,[6] X. Litaudon,[6] R. Kumazawa,[7] H. Kasahara,[7] and EAST Team

[1]*Institute of Plasma Physics, Chinese Academy of Sciences, Hefei 230031, China*
[2]*MIT Plasma Science and Fusion Center, Cambridge, Massachusetts 02139, USA*
[3]*Princeton Plasma Physics Laboratory, Princeton University, Princeton, New Jersey 08543, USA*
[4]*Max-Planck Institute for Plasma Physics, D-85748 Garching, Germany*
[5]*University of Gent, Belgium*
[6]*CEA, IRFM, F-13108 Saint-Paul Lez Durance, France*
[7]*National Institute for Fusion Science, Toki, Japan*

(Received 10 December 2013; accepted 17 February 2014; published online 18 June 2014)

An ion cyclotron range of frequencies (ICRF) system with power up to 6.0 MW and a lower hybrid current drive (LHCD) system up to 4 MW have been applied for heating and current drive experiments in Experimental Advanced Superconducting Tokomak (EAST). Significant progress has been made with ICRF heating and LHCD for realizing the H-mode plasma operation in EAST. During 2010 and 2012 experimental campaigns, ICRF heating experiments were carried out at the fixed frequency of 27MHz, achieving effective ions and electrons heating with the H minority heating (H-MH) mode. The H-MH mode produced good plasma performance, and realized H-mode using ICRF power alone in 2012. In 2010, H-modes were generated and sustained by LHCD alone, where lithium coating and gas puffing near the mouth of the LH launcher were applied to improve the LHCD power coupling and penetration into the core plasmas of H-modes. In 2012, the combination of LHCD and ICRH power extended the H-mode duration up to over 30 s. H-modes with various types of edge localized modes (ELMs) have been achieved with $H_{IPB98}(y, 2)$ ranging from 0.7 to over unity. A brief overview of LHCD and ICRF Heating experiment and their application in achieving H-mode operation during these two campaigns will be presented. © *2014 AIP Publishing LLC*. [http://dx.doi.org/10.1063/1.4884356]

I. INTRODUCTION

Experimental Advanced Superconducting Tokomak (EAST) is a full superconducting device with an advanced configuration in the world,[1–4] starting operation in 2006. Its purpose is to establish the scientific and technological basis for the next generation of tokamak reactors.[5] The design parameters of the EAST device are toroidal field $B_t = 3.5$ T, plasma current $I_p = 1$ MA, major radius $R = 1.7$–1.9 m, minor radius $a = 0.4$–0.45 m, triangularity $\delta = 0.4$–0.7, and elongation κ 0.2–2 for Single-Null (SN) and Double Null (DN) divertor operations.

At the initial operation phase, 2.0 MW at 2.45 GHz (Refs. 6 and 7) and 1.5 MW ICRF system[8,9] were equipped. These systems have been recently upgraded to 4.0 MW and 6.0 MW, respectively. The LHCD launcher and the protection limiters have been modified to better match the plasma boundary shape. Such an LHCD system can deliver a continuous-wave power of 4.0 MW at the frequency of 2.45 GHz. Four 1.5 MW ICRF transmitters in the frequency range of 25–70 MHz were operating in the 2012 experimental campaigns. Two of them powered the I-port antenna and the other two powered the B-port antenna. The Faraday shields of the B-port antennas have been coated with B_4C. With the enhanced heating and current-drive capabilities, EAST achieved reproducible steady-state H-mode plasmas lasting longer than 30 s under a strongly lithium-coated wall condition in the 2012 experimental campaign.

H-mode in EAST was first achieved with LHCD alone in 2010 autumn experimental campaign. The first H-mode with type-III edge localized modes (ELMs)[10] at an H factor of $H_{IPB98}(y,2) \sim 0.8 \pm 0.2$ was obtained at a power level close to the threshold power (~1 MW), predicted by the international tokamak scaling. The reduced recycling by extensive lithium (Li) wall coating was thought to be the key factor to access the H-mode at this power level, together with the good LHCD efficiency expected in such regimes due to good wave penetration and reduced effect of parametric instabilities (PI).[11] In the 2010 autumn campaign, H-mode plasmas by ICRF heating were only accessed together with LH power due to the low ICRF power absorption. In the 2012 campaign, H mode plasmas were achieved by ICRF power alone. These H-modes had type-III edge localized modes (ELMs)[12] and confinement factor $H_{IPB98}(y,2) \sim 0.7 \pm 0.1$. New features of H-mode plasmas have been reliably generated by the combination of LHCD and ICRF power. Furthermore, the H-mode duration has been extended from 6.4 s in 2010 to >30 s in 2012. These H-modes, with approximately several tens of the current

a)Email: bnwan@ipp.ac.cn

diffusion time, are the longest H-mode plasmas in a small-ELM regime in the world. The H-mode discharge shown in Fig. 30 of Refs. 13 and 14 has been achieved by combined LHCD and ICRH input power of ~2.5 MW with small ELMs and $H_{IPB98}(y, 2) \sim 0.8 \pm 0.1$.

II. OVERVIEW OF ICRF HEATING EXPERIMENTS IN D (H) PLASMAS

The performance of ICRF heating has progressed steadily in EAST.[15,16] This is mainly because lithium wall conditioning has been routinely used to reduce both impurity and hydrogen recycling, which helps improve the ICRF power absorption.[15,17] In the 2010 campaign, the lowest hydrogen concentration was ~7% with lithium coating. An example of H minority heating is shown in Fig. 1, where 1.0 MW of ICRF power at 27 MHz was injected from the O and I port two strap antennas into a discharge of $B_{t0} = 2.0$ T and $I_p = 500$ kA. One can clearly see that electron density dropped by about 20% after the ICRF power was applied.[16] The electron temperature was increased by more than 1.0 keV. The stored energy has an increase of 30 kJ.

In the 2012 spring campaign, EAST capabilities had been greatly improved. Graphite tiles on the low heat load area were replaced by molybdenum, except for the divertor regions. This modification together with intensive Li wall coating allowed us to reduce hydrogen concentration in deuterium plasma further, from previous ~10% to ~3%, which allowed more effective ICRF H-minority heating. The heating performance was found to depend on the magnetic field as shown in Fig. 2, where the increment of stored plasma energy due to the ICRF pulse is plotted versus magnetic field strength. For the data shown in the figure, the ICRF power was less than 1.8 MW with the frequency fixed at 27.0 MHz in L-mode plasma. The best results for H-MH mode were obtained at a magnetic field of 1.95 T, and the increase of the stored energy reached 23 kJ using ICRF alone. As shown in Fig. 1 of Ref. 16, at the optimum magnetic field, the resonance layer of Hydrogen is located near the plasma center.

An example of ICRF heated discharge at $B_{t0} = 1.96$ T and $I_p = 500$ kA and hydrogen concentration is about 3% is shown in Fig. 3 where the B and I port antennas were operated in $(0, \pi)$ phasing and RF frequency was 27 MHz. Both ions and electrons heating were observed in the H-minority heating scheme in the deuterium majority plasma. The neutron rate and stored energy were increased when ICRF power was switched on. A significant rise of central ions and electrons temperature measured by X-ray crystal spectrometer was observed. The sawtooth period also increases with the addition of ICRF power (as shown in Fig. 4). As can be seen in Ref. 18, this could be partly due to the stabilization effect from the high-energy populations of H ions created by the H minority heating.

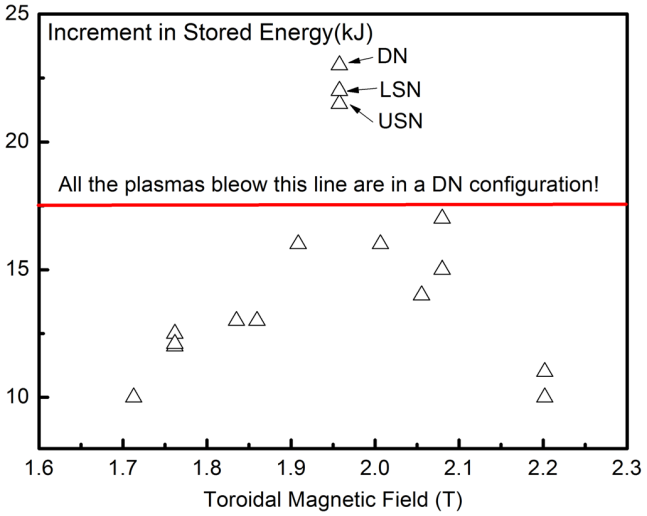

FIG. 2. ICRF heating depended on the magnetic field with plasma density near 2×10^{19} m^{-3}.

III. OPTIMIZATION OF LHCD IN EAST

Lower hybrid current drive (LHCD)[19,20] plays a key role in controlling current profile in tokamak experiments aimed at achieving important goals relevant to fusion plasma. LHW-plasma coupling depends strongly on the density at the mouth of the grill. Experiments have been performed to optimize the coupling of the LHW power to the plasma. The experiments were carried out through a scan of

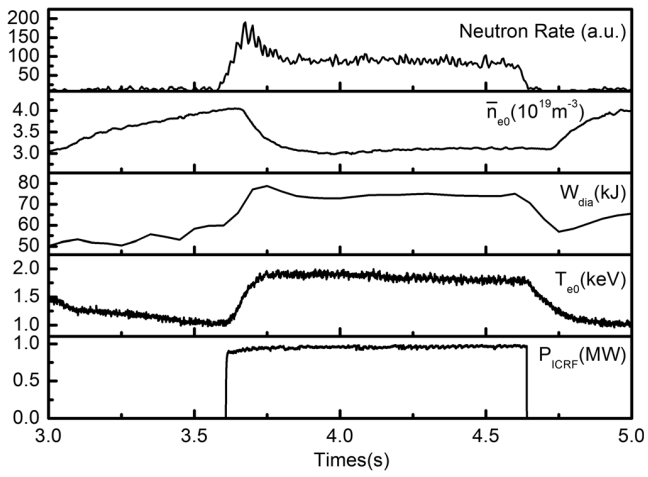

FIG. 1. An example of ICRF heating in EAST from the 2010 campaign with 1.0 MW ICRF power at 27 MHz injected from the O- and I- port antennas.

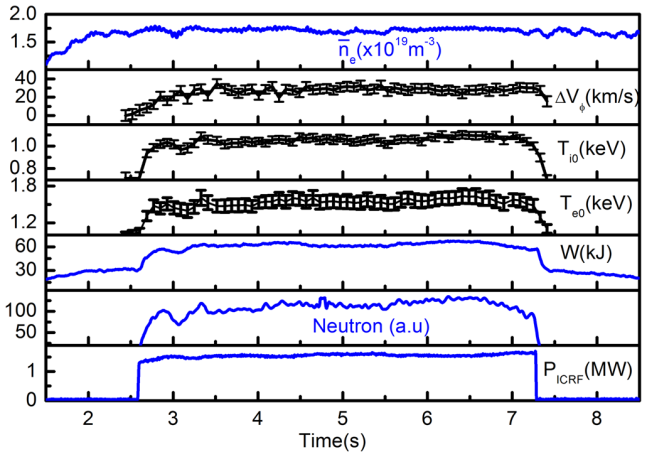

FIG. 3. An example of ICRF Heating plasma discharge showing effective electron and ions heating. Total ICRF power was 1.7 MW injected from the B- and I- port antennas.

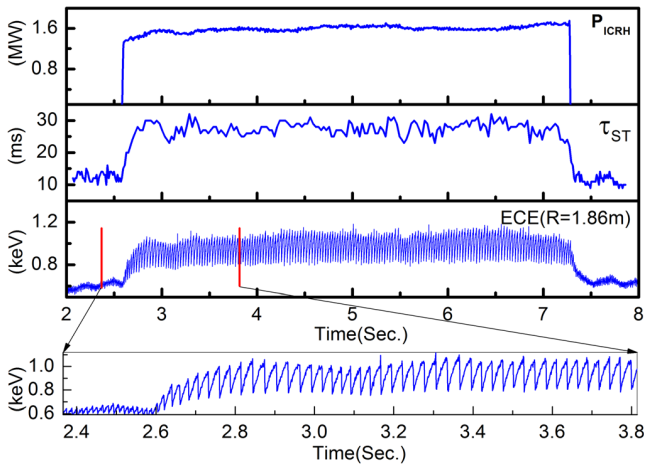

FIG. 4. Sawtooth behavior in an ICRF H-minority heated D majority plasma.

the gap between the last closed flux surface (LCFS) and the mouth of the LHCD launcher. In order to improve LHW-plasma coupling, two gas pipes covering the total grill in the poloidal direction have been installed near the LHW antenna in EAST. The toroidal angle between the grill and the pipes are about 33°. Effective coupling for LHW and relevant questions mentioned in Ref. 21 have been further studied[22] in EAST after the recent upgrade. By optimizing the shape of the LH grill, the misalignment of between poloidal limiter and the LH grill has been nearly eliminated and the coupling of LHW has improved. But the coupling deteriorates as the transition of L-H occurs due to the steep gradient density profile in H-mode, which lowers the density at the grill mouth. Fortunately, gas puffing near the LH grill can reverse the local density depletion.

Experiments of gas puffing from the electron-side and the ion-side on LHW-plasma interaction were first performed in EAST.[23,24] The results suggest that gas puffing from the electron-side is more efficient for improving LHW-plasma coupling. As shown in Figs. 5(a) and 5(b), the electron density at the last closed flux surface (LCFS) and the reflection coefficients (RCs) are plotted vs. different gas flow rate.

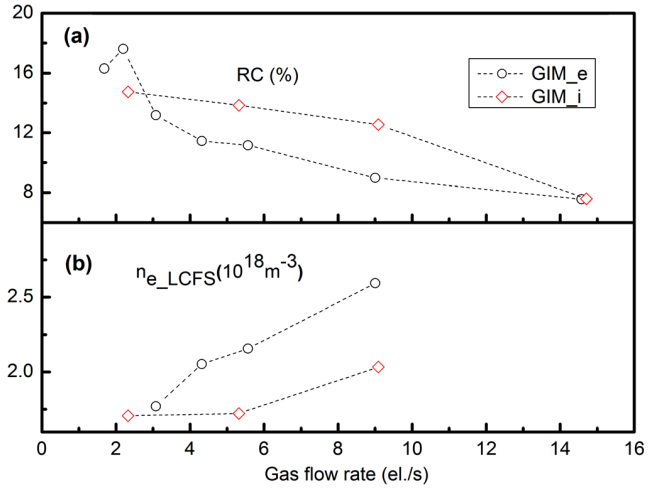

FIG. 5. Comparison of the effect of gas puffing from different side on the LHW coupling and the electron density at the last closed flux surface: (a) RC vs gas flow rate; (b) n_{e_LCFS} vs Gas flow rate.

However, the local edge density during ICRF power can be reduced further.[21] Such ICRF modifications are stronger at higher ICRF power operations. RF sheaths can play some role in affecting the local edge density. The changes in LHW coupling associated with different ICRF antennas have been explored. In some cases, the coupling on the lower rows of the LH grill was seen to be affected, possibly due to magnetic connection between ICRF antennas and the LH grill. To reduce the ICRF effect, the ICRF antennas at the O-port will be moved from the O-port to the B-port in the 2012 experimental campaign.

High density is a challenge to the LHCD experiments in H-mode discharges. In high density plasmas, lower hybrid (LH) waves have been observed to dissipate the power in the plasma periphery and degrade the LHCD efficiency. Recent high density experiments on FTU have shown that LH wave's efficiency is recovered and measured spectral broadening of launched wave reduced, by increasing peripheral temperature[11] as expected by the theory that predicts a reduced effect of parametric instability.[25] Different mechanisms can concur in preventing LH wave penetration at high density, for example, collisional absorption (CA),[26] PI,[11,25,27] scattering from density fluctuations (SDF),[28–30] and so on. The broadening of the LH power spectra[31] vs. the parallel refractive index N//, produced by PI, results in spurious LH power absorption at the edge, via Landau damping. The relevant experiments performed in EAST indicated that the effect of current drive with gas puffing is much better with strong lithium coating than that with poor lithium coating. This observation is consistent with the previous studies that lithium coating is beneficial to increase CD efficiency at high density, due to the low recycling and high edge temperature in the lithium condition. At similar lithium coating, the current drive effect with supersonic molecular beam injection (SMBI) is worse than that with gas puffing. The mechanism for this observation is unclear. A possible explanation is that the SMBI experiments produce higher SDF due to the larger density fluctuation in the edge region (Fig. 6). In addition, in the SMBI case, a relative high neutral deuterium

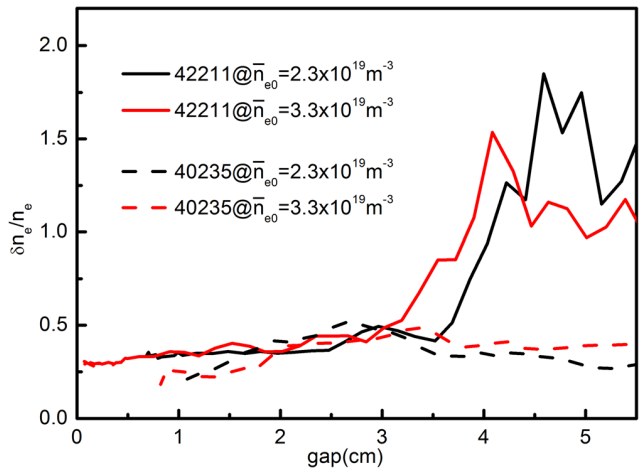

FIG. 6. Comparison of density fluctuation profile in the SOL under different conditions (0 means the position of the LCFS): 40235 (gas puffing, strong lithiation, PLH = 1.5 MW); 42211 (SMBI, strong lithiation, PLH = 1.2 MW).

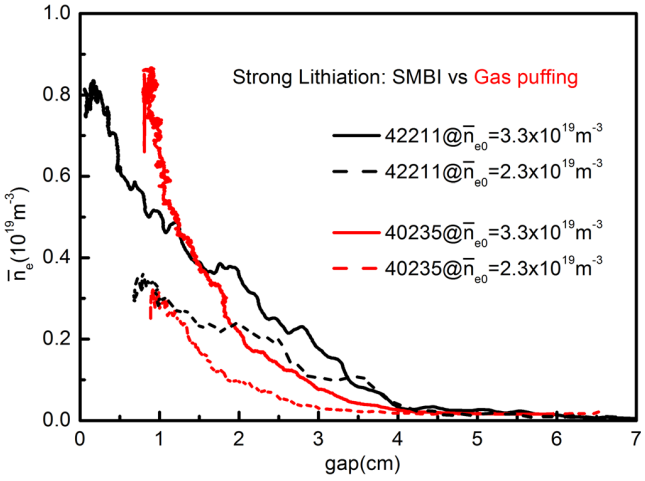

FIG. 7. Comparison of density profile in the SOL under different conditions (0 means the position of the LCFS); 40235 (gas puffing, strong lithiation, PLH = 1.5 MW); 42211 (SMBI, strong lithiation, PLH = 1.2 MW).

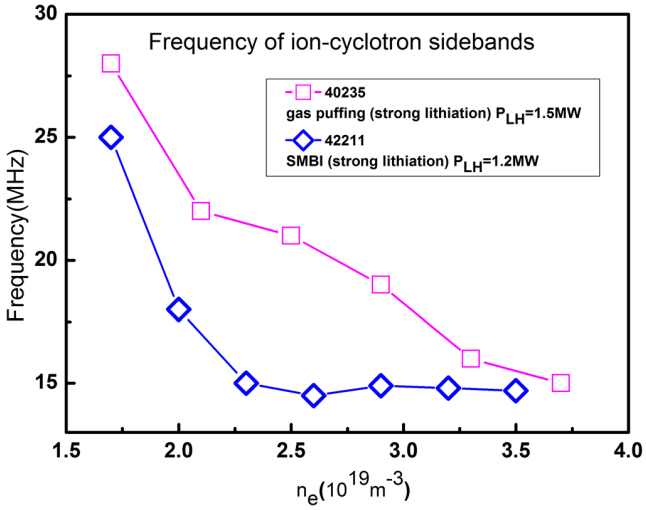

FIG. 9. Comparison of frequency of IC sidebands under different conditions.

radiation is observed.[22] This may result in high density in the edge (Fig. 7), leading to the low CD effect possibly due to PDI or CA. As shown in Fig. 8, a lower temperature may occur at a higher deuterium radiation, hence being more subject to PDI behavior. This is in good agreement with the relationship between deuterium radiation and CD efficiency.

Wave accessibility and PDI have been suggested as possible explanations for the density limits observed on previous LHCD experiments.[26,32,33] PDI induced by LH wave power injection is a four wave coupling process. The wavenumber of the daughter LH wave may upshift substantially, thereby reducing the current drive efficiency. Since the magnetic toroidal field and the LHW spectrum are fixed in the experiments, the discrepancy in sharp decay of bremsstrahlung emission is not due to wave accessibility. In addition, the dependences of CD effect on density are nearly consistent with the frequency of ion-cyclotron (IC) sideband [Fig. 9], measured by a RF loop antenna located outside the machine, implying the sharp decay of HXR counts observed in high density LHCD experiments is correlated with PDI.[22] As described in Refs. 34 and 35, n, Nonlinear interactions involving the overall spectra of the launched and noise LH waves at the plasma edge play indeed an important role in determining the power absorption of the RF power externally launched in tokamak plasmas. In addition, higher convective losses occur due to the bigger shifts in frequency and N// of the sidebands.[31]

Comparing the experimental data for different current and magnetic field, experiments also show that CD effect is better in higher plasma current or higher toroidal magnetic field, in agreement with studies in Tore-Supra. This is because high plasma current is favorable to increase temperature, hence improving CD efficiency. The effect of magnetic field on efficiency is mainly ascribed to wave accessibility condition. By further comparing the HXR counts in L- and H-mode, it appears that at the same density, the CD efficiency in H-mode is larger than that in L-mode, indicating profile dependence or edge dependence in CD efficiency.

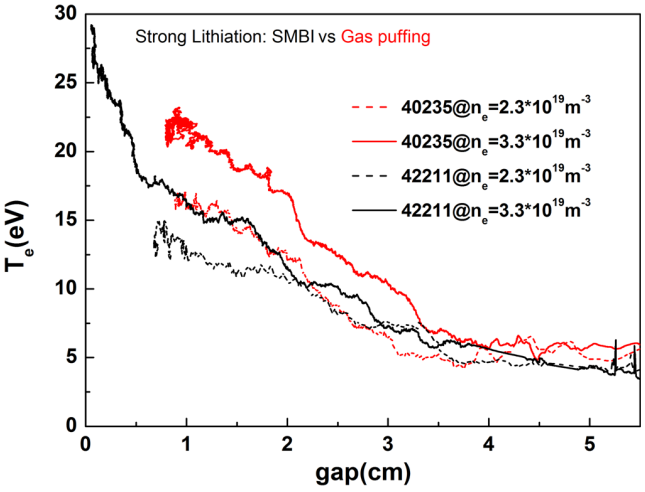

FIG. 8. Comparison of temperature profile in the SOL under different conditions (0 means the position of the LCFS); 40235 (gas puffing, strong lithiation, PLH = 1.5 MW); 42211 (SMBI, strong lithiation, PLH = 1.2 MW).

IV. APPLICATION OF LHCD AND ICRF HEATING IN H MODE EXPERIMENTS

With H minority heating mode in D(H) plasma, for the first time, ICRF heated H mode have been reproducibly achieved with injected RF power of ~1.7 MW launched by the B- and I-port antennas. The H-mode shown in Fig. 10 started with a short ELM-free period, lasting ~500 ms, followed by type III ELMs (Figure 9(a)). The ELM frequency varies from 200 Hz to 500 Hz (Figure 4(b) of Ref. 11). Confinement times for the H-mode discharges were in the range of 110 ms to 150 ms for 1.7 MW of total heating power at 500 kA. The H factor, $H_{IPB98}(y,2)$, for the L mode plasma just before the transitions was about 0.5 and then it rose up to 0.7 ± 0.1.

As shown in Fig. 11, the first ELMy H-mode plasma with type-III edge localized modes at an H factor of $H_{98IPB\ (y,\ 2)} \sim 1$ were obtained with only 1 MW of LHW power in 2010 experimental campaign. To access H-mode

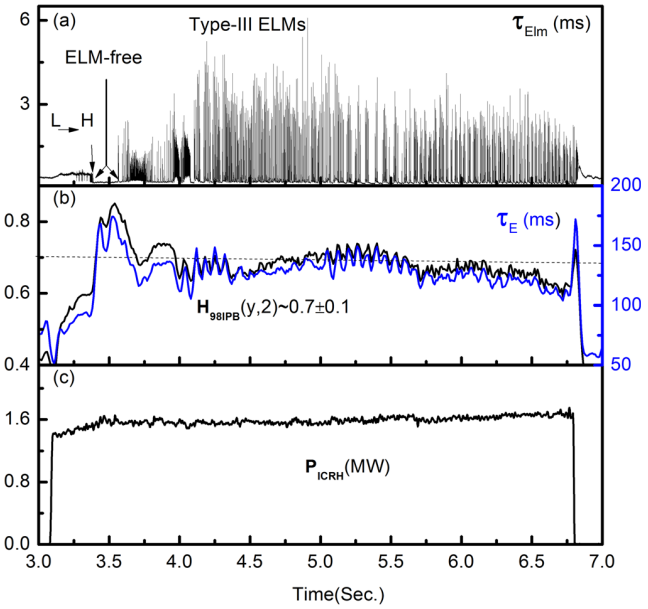

FIG. 10. An example of ICRF heated H mode from the 2012 campaign with 1.7 MW of ICRF power injected from the B- and I- port antennas.

at this power level, extensive Li wall coating by evaporation and Li powder injection were found necessary. With increasing accumulation of deposited Li, the H-mode duration was gradually extended up to 3.6 s. The threshold power for H-mode access follows the international tokamak scaling.

H mode experiments have been performed in EAST to identify different regimes of H-mode operation and different ELMy characteristics. As discussed in Ref. 10, the lithium injection plays a very important role in triggering the L-H transition. Every day before experimental operation, Lithium were evaporated for 1–2 h using two ovens at toroidally symmetric midplane positions. The application of Li significantly

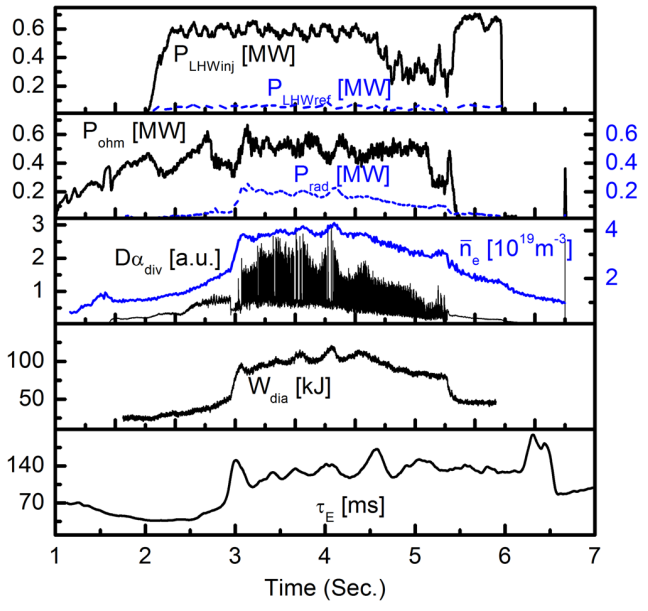

FIG. 11. An example of LHCD H mode from the 2010 campaign with 1.0 MW of LHW power.

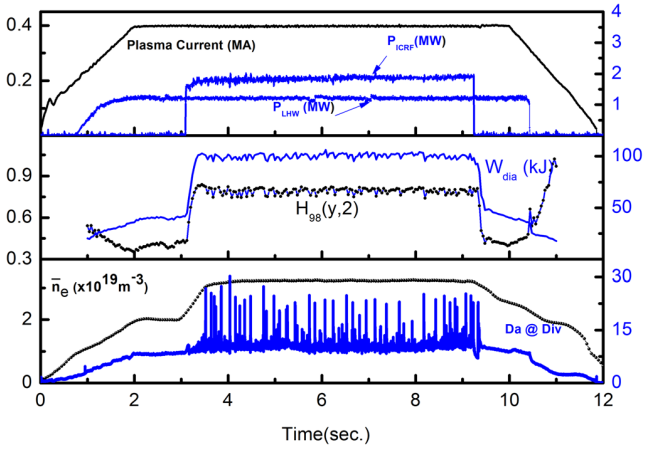

FIG. 12. Stationary H-mode with mixed type-I and small ELMs.

suppressed oxygen impurities but had little effect on carbon. The H/(D+H) ratio, however, was progressively reduced up to ~3% in deuterium plasmas. Considering isotope scaling, the lower H/(D+H) ratio could help us to reduce the power threshold. In the 2010 experimental campaign, the H mode obtained were mostly type-III ELMs H mode. In the 2012 experimental campaign, the improved capabilities have enabled study of new features of H-mode physics in RF dominated regimes. EAST has achieved H modes with different type ELMs, as described in the following:

a) By increasing ICRF heating power in LHW driven plasmas, steady-state ELMy H-modes with mixed type-I and small ELMs were achieved as shown in Fig. 12. This H-mode regime was obtained at low density ($n_e/n_G \sim 0.46$) by applying 1.2 MW LHCD and 1.6 MW ICRF in LSN configuration with lower triangularity $\delta \sim 0.48$. The H-mode operation appeared to be more stable with LSN configuration. It could be due to the strong particle control provided by the internal cryogenic pump beneath the lower outer divertor plate.

b) By reducing plasma density at $I_p \sim 0.3$ MA and increasing ICRF heating power, type-I ELMy dominated H modes with good confinement, i.e., $H_{IPB98}(y,2) \sim 1$, were achieved. Fig. 13 shows such a typical H-mode discharge

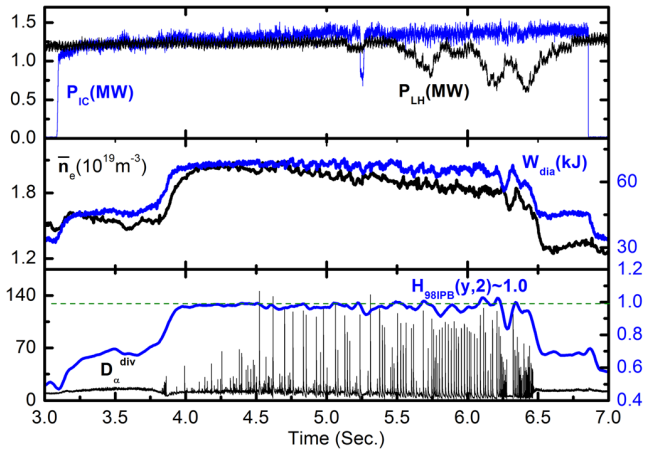

FIG. 13. Type-I ELMy H mode with $H_{IPB98}(y,2) \sim 1$.

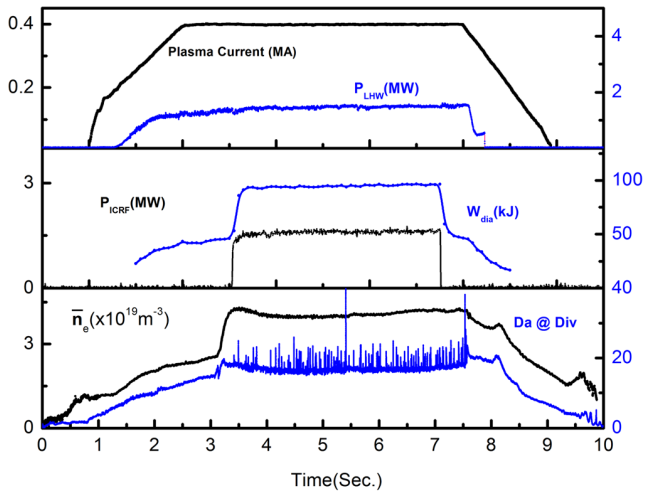

FIG. 14. H mode with an Enhanced D_α emission, irregular ELMs.

with the central-line-averaged density at $n_e/n_G \sim 0.4$ during the H-mode period. Type-I ELMs have been observed to produce substantial loss, up to ~10%, of the plasma-stored energy.

c) By increasing the density to $n_e/n_G \sim 0.62$, an enhanced Da H-mode regime was obtained with LSN configuration and lower triangularity $\delta \sim 0.43$. The regime was characterized by two coherent modes[12] at the plasma edge with frequency ~30 kHz and ~200 kHz, together with enhanced D_α emission and small ELMs, as shown in Fig. 14.

V. SUMMARY AND NEAR FUTURE PLAN

In summary, significant progress has been made on EAST toward long-pulse high-performance operation. EAST is now undertaking an extensive upgrade for high-power and longer-pulse operation. Fig. 15 shows the arrangement of the upgraded auxiliary heating systems on EAST. After completing this upgrade, EAST will be equipped with more than 30 MW CW H&CD power and ITER-like W mono-block divertor. These new capabilities will make EAST a unique facility to address some critical issues related to steady-state H-mode physics in RF dominated regimes for long-pulse operations under ITER relevant conditions in the near future.

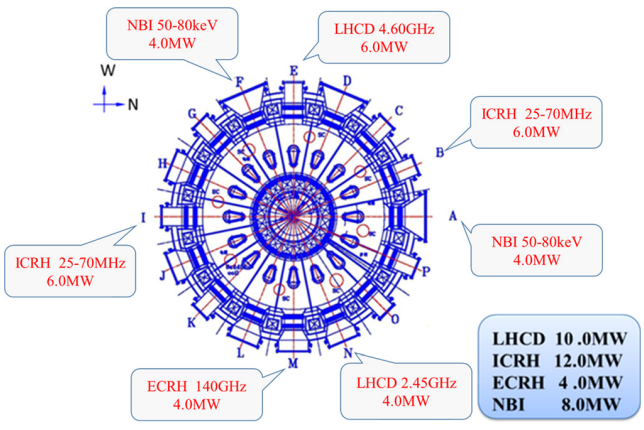

FIG. 15. The arrangement of auxiliary heating systems on EAST.

ACKNOWLEDGMENTS

The authors would like to acknowledge the support of and EAST operation and diagnostics group. This work was supported partially by the National Natural Science Foundation of China under Grant Nos. 11105179, 11375235, 11175206, 10725523, 10721505, 10990210, 10990212, 11075182, 11021565, 11075181, 11175208 and sponsored in part by National Magnetic Confinement Fusion Science Program of China under Contract Nos. 2011GB101000, 2013GB112004, 2011GB101004, 2011GB107001, 2013GB106000, 2013GB107003 and 2010GB104001, and by JSPS-NRF-NSFC A3 Foresight Program in the field of Plasma Physics (NSFC No. 11261140328).

[1]Y. Wan and J. Li, P. Weng for EAST, GA, and PPPL Team, "Overview progress and future plan of EAST Project," in *Proceedings of the 21th International Conference on Fusion energy* (Chengdu, China 2006) (Vienna, IAEA) OV/1-1http://wwwnaweb.iaea.org/napc/physics/fec/fec2006/talks/t_ov_1-1.pdf.

[2]B. Wan for EAST and HT-7 Team and International Collaborators 2008, in *Proceedings 22nd IAEA Conference on Fusion Energy* (Geneva, Switzerland, 2008) http://wwwnaweb.iaea.org/napc/physics/FEC/FEC2008/papers/ov_3-4.pdf.

[3]B. Wan, J. Li, Y. Wu, for EAST, HT-7, FDS Teams, and International Collaborators, Fusion Eng. Des. **85**, 1048 (2010).

[4]B. N. Wan and International Collaborators, Nucl. Fusion **49**, 104011 (2009).

[5]Y. Wan, HT-7 Team, and HT-7U Team, Nucl. Fusion **40**, 1057 (2000).

[6]L. M. Zhao, J. F. Shan, and F. K. Liu, Plasma Sci. Technol. **12**, 118 (2010).

[7]B. J. Ding, Y. L. Qin, W. K. Li, M. H. Li, E. H. Kong, L. Zhang, A. Ekedahl, Y. Peysson, J. Decker, M. Wang, H. D. Xu1, H. C. Hu, G. S. Xu, J. F. Shan, F. K. Liu, Y. P. Zhao, B. N. Wan, J. G. Li, and EAST Group, Phys. Plasma **18**, 082510 (2011).

[8]J. Li and B. Wan for EAST Team and International Collaborators, Nucl. Fusion **51**, 094007 (2011).

[9]X. J. Zhang, Y. P. Zhao, B. N. Wan, J. G. Li, Y. Z. Mao, S. Yuan, D. Y. Xue, C. M. Qin, C. H. Wang, Y. Lin, B. J. Ding, and EAST Group, in *Proceedings of the 23rd International Conference on Fusion Energy* (Daejeon, Republic of Korea, 2010) (Vienna, IAEA) http://www-pub.iaea.org/mtcd/meetings/PDFplus/2010/cn180/cn180papers/exwp7-30.pdf.

[10]G. S. Xu, B. N. Wan, J. G. Li, X. Z. Gong, J. S. Hu, J. F. Shan, H. Li, D. K. Mansfield, D. A. Humphreys, and V. Naulin for EAST Team and International Collaborators, Nucl. Fusion **51**, 072001 (2011).

[11]R. Cesario, L. Amicucci, A. Cardinali, C. Castaldo, M. Marinucci, L. Panaccione, F. Santini, O. Tudisco, M. L. Apicella, G. Calabro, C. Cianfarani, D. Frigione, A. Galli, G. Mazzitelli, C. Mazzotta, V. Pericoli, G. Schettini, A. A. Tuccillo, and the FTU Team, Nat. Commun. **1**, Art. No. 55 (2013).

[12]X. J. Zhang, Y. P. Zhao, B. N. Wan, X. Z. Gong, J. G. Li, Y. Lin, C. M. Qin, G. Taylor, G. S. Xu, Y. W. Sun, B. X. Gao, J. P. Qian, F. D. Wang, B. Lu, C. Luo, L. Zhang, L. Q. Hu, Y. T. Song, C. X. Yu, W. D. Liu, S. Wukitch, J. R. Wilson, and J. C. Hosea, Nucl. Fusion **53**, 023004 (2013).

[13]B. Wan, J. Li, H. Guo, Y. Liang, G. Xu, X. Gong for the EAST Team, and International Collaborators, Nucl. Fusion **53**, 104006 (2013).

[14]J. Li, H. Y. Guo, B. N. Wan, X. Z. Gong, Y. F. Liang, G. S. Xu, K. F. Gan, J. S. Hu, H. Q. Wang, L. Wang, L. Zeng, Y. P. Zhao, P. Denner, G. L. Jackson, A. Loarte, R. Maingi, J. E. Menard, M. Rack, and X. L. Zou, Nature Phys. **9**, 817–821 (2013).

[15]Z. Xinjun, Z. Yanping, M. Yuzhou, Y. Shuai, X. Diye, W. Lei, D. Jiayi, Q. Chengming, J. U. Songqing, C. Yan, W. Chenghao, S. Junsong, S. Yuntao, and L. Yijun, Plasma Sci. Technol. **13**, 172 (2011).

[16]X. J. Zhang, Y. P. Zhao, B. N. Wan, X. Z. Gong, Y. Z. Mao, S. Yuan, D. Y. Xue, L. Wang, C. M. Qin, S. Q. Ju, Y. Chen, J. P. Qian, L. Hu, J. G. Li,

Y. T. Song, Y. Lin, S. Wukitch, J. M. Noterdaeme, R. Kumazawa, T. Seki, K. Saito, and H. Kasahara, Nucl. Fusion **52**, 032002 (2012).
[17]G. Z. Zuo, J. S. Hu, S. Zhen, J. G. Li, D. K. Mansfield, B. Cao, J. H. Wu, L. E. Zakharov, and the EAST Team, Plasma Phys. Controlled Fusion **54**, 015014 (2012).
[18]F. Porcelli, Plasma Phys. Controlled Fusion **33**(13), 1601 (1991).
[19]N. J. Fisch, Phys. Rev. Lett. **41**, 873 (1978).
[20]S. Bernabei, C. Daughney, P. Efthimion, W. Hooke, J. Hosea, F. Jobes, A. Martin, E. Mazzucato, E. Meservey, R. Motley, J. Stevens, S. Von Goeler, and R. Wilson, Phys. Rev. Lett. **49**, 1255 (1982).
[21]E. H. Kong, T. Zhang, B. J. Ding, L. Liu, C. M. Qin, X. Z. Gong, Z. G. Wu, J. F. Shan, F. K. Liu, M. H. Li, L. Zhang, M. Wang, H. D. Xu, Y. P. Zhao, L. M. Zhao, J. Q. Feng, Y. Yang, H. Jia, H. C. Hu, X. J. Wang, J. H. Wu, Z. X. He, and EAST Team, Plasma Phys. Controlled Fusion **54**, 105003 (2012).
[22]E. H. Kong, B. J. Ding, L. Zhang, L. Liu, C. M. Qin, X. Z. Gong, G. S. Xu, X. J. Zhang, Z. G. Wu, H. Q. Wang, M. H. Li, W. Wei, Y. C. Li, L. Xu, J. H. Wu, Z. X. He, J. F. Shan, F. K. Liu, M. Wang, H. D. Xu, Y. P. Zhao, L. M. Zhao, J. Q. Feng, Y. Yang, H. Jia, H. C. Hu, X. J. Wang, D. J. Wu, and the EAST Team, Plasma Phys. Controlled Fusion **55**, 065007 (2013).
[23]B. J. Ding, E. H. Kong, M. H. Li, Lei Zhang, W. Wei, M. Wang, H. D. Xu, Y. C. Li, B. L. Ling, Q. Zang, G. S. Xu, X. F. Han, H. L. Zhao, L. Zhang, L. M. Zhao, H. C. Hu, Y. Yang, L. Liu, A. Ekedahl, M. Goniche, R. Cesario, Y. Peysson, J. Decker, V. Basiuk, P. Huynh, J. Artaud, F. Imbeaux, J. F. Shan, F. K. Liu, Y. P. Zhao, X. Z. Gong, L. Q. Hu, X. Gao, H. Y. Guo, B. N. Wan, J. G. Li, and the EAST Team, Nucl. Fusion **53**, 113027 (2013).
[24]B. J. Ding, E. H. Kong, T. Zhang, A. Ekedahl, M. H. Li, L. Zhang, W. Wei, Y. C. Li, J. H. Wu, G. S. Xu, H. L. Zhao, M. Wang, X. Z. Gong, J. F. Shan, F. K. Liu, and EAST Team, Phys. Plasmas **20**, 102504 (2013).
[25]R. Cesario, A. Cardinali, C. Castaldo, F. Paoletti, and D. Mazon, Phys. Rev. Lett. **92**(17) 175002 (2004).
[26]P. T. Bonoli and R. C. Englade, Phys. Fluids **29**, 2937 (1986).
[27]R. Cesario, L. Amicucci, C. Castaldo, M. Kempenaars, S. Jachmich, J. Mailloux, O. Tudisco, A. Galli, A. Krivska, and JET-EFDA contributors, Plasma Phys. Controlled Fusion **53**, 085011 (2011).
[28]E. Ott, Phys. Fluids **22**, 1732 (1979).
[29]P. L. Andrews and F. W. Perkins, Phys. Fluids **26**, 2546 (1983).
[30]Y. Peysson, L. Decker, L. Joan Decker, L. Morini, and S. Coda, Plasma Phys. Controlled Fusion **53**, 124028 (2011).
[31]R. Cesario, A. Cardinali, C. Castaldo, F. Paoletti, W. Fundamenski, S. Hacquin, and the JET-EFDA workprogramme contributors, Nucl. Fusion **46**, 462 (2006).
[32]Y. Takase, M. Porkolab, J. J. Schuss, R. L. Watterson, C. L. Fiore, R. E. Slusher, and C. M. Surko, Phys. Fluids **28**, 983 (1985).
[33]W. Hooke, Plasma Phys. Controlled Fusion **26**, 133 (1984).
[34]C. Castaldo, E. Lazzaro, M. Lontano, and A. M. Sergeev, Phys. Lett. A **230**(5–6), 336 (1997).
[35]F. Napoli, C. Castaldo, R. Cesario, and G. Schettini, Plasma Phys. Controlled Fusion **55**(9), 095004 (2013).